UHF RFID Tag Design using Theory of Characteristics Modes for Platform-tolerant and Harsh Metallic Environments

Abubakar Sharif[1,2], *Member, IEEE,* Jun Ouyang[2], *Member, IEEE,* Ali Raza[1], Sajjad Hussain[2], Muhammad Nasir[3], Kamran Arshad[4], *Senior Member, IEEE,* Khaled Assaleh[4], *Senior Member, IEEE*, Naeem Ramzan, *Senior Member, IEEE* Muhammad Ali Imran[5], *Senior Member, IEEE* and Qammer H. Abbasi[5], *Senior Member, IEEE*

***Abstract*—This paper presents a wideband, long-range RFID tag antenna design with platform tolerant features using characteristic mode analysis (CMA). The proposed design consists of a two-layer structure, that are separated by an air gap. The upper layer consists of T-match and dual loop-based meandered antenna optimized for achieving long read range characteristics in free space/low permittivity dielectrics. The second layer consists of multi-resonant strips printed on a grounded substrate carefully designed using CMA for producing multi-resonant modes in the required UHF RFID band. The multi-resonant strips help in achieving wide bandwidth and isolation between different environment surfaces. This tag antenna provides a wide bandwidth ranging from 900 – 940 MHz that covers both the US UHF RFID band (902 – 928 MHz) and the upper European UHF RFID band (915 – 921 MHz). Moreover, this design achieved a read range of 14.7 m in free space, 14 m on a metal plate, and 13 m on wood, and glass. Furthermore, the proposed antenna was also tested in harsh metal environments such as car number plates and cargo metallic containers. Therefore, the proposed tag can be used for tagging metallic containers, wood containers, and other harsh platforms for cargo management, Asset tracking, supply chain visibility, and Internet of Things (IoT) Applications.**

***Index Terms*— Characteristics Mode Analysis, Harsh Metallic Environments, platform-tolerant, Radio frequency identification (RFID), Tag antenna design, Impedance matching**

I. Introduction

IoT and RFID are emerging technologies that are transforming our earth into a smart planet by providing outstanding applications such as smart city, smart supply chain, Fleet management, traffic monitoring, smart healthcare, and so forth. RFID technology is considered to be an excellent short-range IoT solution [1]–[4]. Passive UHF RFID tags are most promising due to their long read range and low-cost tag structures. However, UHF RFID tags are sensitive toward different tagging surfaces such as metals and other high permittivity substances. Metallic surfaces pose severe degradation in the performance of RFID tags due to image currents cancellation effects (due to different boundary conditions) that reduce radiation efficiency and hence worsen impedance matching and read range of UHF tags. The challenge of tagging surfaces is magnified further for large, thick, heavy metals and wood containers [5]–[9].

Recent researches have reported several techniques and tag designs to overcome the metallic effects [10]. A compact, multilayer tag with a stacked planar inverted L antenna (PILA) structure has been proposed in [11]. This multilayer PILA structure provides enhanced capacitance that eventually reduces the tag resonance frequency down to the UHF RFID band. Although this PILA design offer compactness, however, the three-layered structure makes it a bit complex and difficult to fabricate. Moreover, this PILA design offers a 7.25 m read range (with 4W-EIRP) and narrow bandwidth. A shorted patch tag antenna with multiple slots was proposed in [12]. This shorted patch was composed of a patch-like structure with two I-shaped slots that are shorted to the ground plane. This design gives a read range of 8.1 m with a relatively narrow bandwidth. In [13], a double-layer patch antenna with a rectangular matching loop was proposed. This double-layered design offered a 4 m read range and cover the whole UHF RFID band (860 – 960 MHz).

Another planar Inverted-F antenna (PIFA) based tag antenna has been proposed in [14]. This antenna achieved post-manufacturing tuning capability with the implantation of lumped elements. Although this tag antenna has a smaller dimension 29.8 × 29.8 × 0.813 mm^3. However, it offers a very

(Corresponding author: Qammer H. Abbasi)

Abubakar Sharif and Jun Ouyang are with School of Electronic Science and Engineering, University of Electronic Science and Technology of China (UESTC). (email: sharifuestc@gmail.com,yjou@uestc.edu.cn)

Abubakar Sharif is also with Department of Electrical Engineering and Technology, Government College University Faisalabad.

Ali Raza is with Department of Electrical Engineering and Technology, Government College University Faisalabad.

Sajjad Hussain is with School of Physics, University of Electronic Science and Technology of China.

Muhammad Nasir is with Electrical Engineering department, university of Engineering and Technology Lahore.

Muhammad Ali Imran and Qammer H. Abbasi are with James Watt School of Engineering, University of Glasgow, Glasgow G12 8QQ, U.K. (e-mail: muhammad.imran@glasgow.ac.uk; qammer.abbasi@glasgow.ac.uk).

Kamran Arshad is with College of Engineering and IT, Ajman University, Ajman, United Arab Emirates. (e-mail:k.arshad@ajman.ac.ae)

Khaled Assaleh is currently the Vice Chancellor for Academic Affairs and a Professor of Electrical Engineering at Ajman University, Ajman, United Arab Emirates. (e-mail:k.assaleh@ajman.ac.ae)

Naeem Ramzan is with School of Computing, Engineering, and Physical Sciences, University of the West of Scotland, Paisley PA1 2BE, UK.

small bandwidth and read range of 3.6 m after mounting on a 10 × 10 cm^2 metal plate. In [15], a differential coplanar feedline-based folded patch antenna was proposed for metal mounting. This folded patch incorporates several slots for tuning and impedance matching mechanisms. Although, this tag design has a small footprint (30 mm × 25 mm × 3.0 mm), however, it poses a complex, difficult-to-fabricate structure along with a small bandwidth and 8.9 m read range. A cavity-type UHF RFID tag antenna with the longest read range of 26 m has been proposed in [16]. The tag design is integrated into a plastic cover made of Polylactic Acid (PLA) with ϵ_r= 1.3. Although, this cavity-type tag antenna poses a long read range, however at the cost of a very large footprint (140 × 60 × 10 mm^3) and complex structure. Moreover, this cavity tag has very low bandwidth.

There were several techniques and methods were reported in the literature [17]. However, we utilize CMA for the analysis and design of the proposed tag antenna. In [18], a planar pyramid-shaped dual-polarized tag antenna has been proposed using CMA. The pyramid tag consists of a bowtie structure with shorting stubs and slots. This tag has low bandwidth and 5.5 mm and 8.5 mm read range over low permittivity dielectrics and metal plates, respectively. A platform tolerant tag antenna with tunable features has been proposed. This tag consists of folded dipole and small loop antenna proximity coupled with the main radiating element. This tag design poses a read range of 4.5 mm and 6.5 mm on low-permittivity materials and metal plates, respectively[19].

A single-layer tag antenna was designed and optimized using CMA. This tag design consists of a meandered loop and radiating patch. Although, this tag design has a read range of 6.1 m and 14.1 m over the metal plate and low-permittivity dielectric surfaces. However, this tag design uses a 3 mm thick substrate, which makes it hefty for many applications [20].

Following the previous statements, the original contributions of our work are:

1. Design guidelines of a platform tolerant antenna using characteristics modes with in-depth analysis and physical insight for antenna designing.
2. The different loop antenna is used to provide a better impedance match and helps to reduce the size of the antenna further.
3. Also, we propose a different set of parallel strips using characteristic modes to create some more resonant modes in required RFID bands.
4. The estimation of the read range of the prototype using Tagformance Pro setup (Which uses turn-on power measurements). Different subjects with different physical compositions were used for read range testing in order to demonstrate the robustness of our solution.
5. The performance of the fabricated tag is tested further in indoor and outdoor environments.
6. The performance of the tag is tested using different widths and sizes of metal plates.

II. Concept and Design

A. Theory of Characteristics Modes

Characteristic modes (CM Modes) are current modes of any arbitrary shaped conducting objects that can be calculated numerically. These CM modes are independent of any excitation or feeding source. CM modes are totally depending on the shape and size of conducting objects. Likewise, characteristic modes (CM) can be attained by solving eigenvalue equations obtained from the Method of Moments (MoM) based impedance matrix as follows [21], [22]:

$$X\left(\vec{J}_n\right) = \lambda_n R\left(\vec{J}_n\right) \tag{1}$$

Where λ_n are the eigenvalues, $\vec{J}_n$ are eigen currents or eigen functions, and R and X are real and imaginary components of MoM impedance matrix, respectively.

B. Proposed Tag Antenna Design using Characteristics Modes Analysis

Fig. 1 shows the initial configuration of the proposed tag design, which was designed and optimized for free space/low permittivity surfaces. This basic configuration was based on T-match, dual nested loop, and meandered dipole-based configuration that provides a good impedance match for free space as well as low-permittivity substrates. The meandered dipole also contains a capacitive end that further reduces the size of the proposed tag design. In order to investigate it further, we conducted a characteristics mode analysis of the proposed single layer tag in free space. The eigenvalue plot of the single-layer tag (SLT) configuration is depicted in Fig. 2. This SLT configuration has one mode radiating around 915 MHz that lies in the US UHF RFID band. The second mode is resonating around 840 MHz, which is not useful for RFID perspective.

Therefore, the SLT configuration is useful for free space/low permittivity dielectric materials. However, the SLT is not good for metallic surfaces and high permittivity materials, since it was fabricated on a 0.5 mm FR4 substrate. This SLT tag does not provide good bandwidth or impedance match on metals as its substrate thickness is very small. In order to sort the aforementioned issue, we proposed a second layer consisting of parallel multi-resonant strips printed over a grounded substrate as shown in Fig. 3.

The multi-resonant strips (MRS) are parasitic elements that can able to excite multiple resonant modes. Those multi-resonant modes are able to enhance the bandwidth of the proposed tag when MRS will be placed in proximity of SLT. The length of the second layer substrate is kept the same as the SLT layer. The length, width, and gap between MRS are optimized using CST Microwave studio to get more number of resonating modes in the required RFID band. Two different widths of MRS were used. The first MRS has a 2.5 mm width, while the second MRS has a 2 mm width, and each MRS has a 1 mm, and 0.5 mm gap.

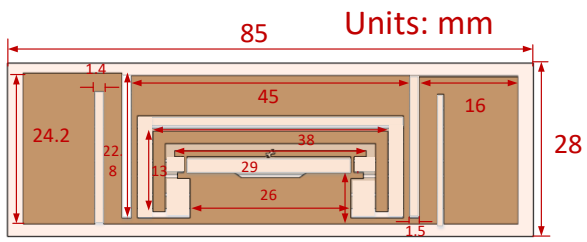

Fig. 1. Detailed dimensions (in millimeters (mm)) and configuration of Initial single-layer design.

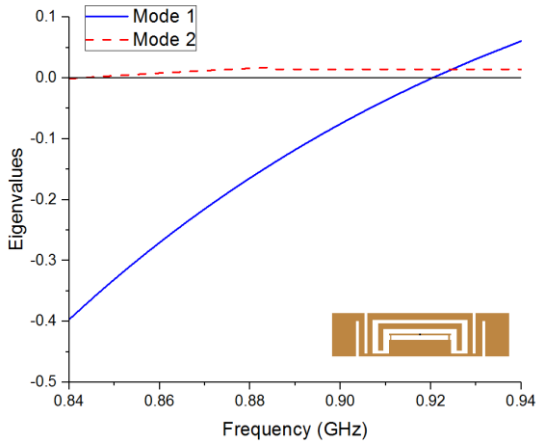

Fig. 2. Eigenvalues plot of the single-layer configuration of proposed tag design.

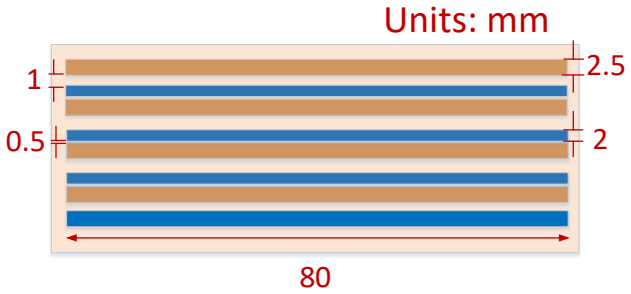

Fig. 3. Detailed dimensions (in millimeters (mm)) of multi-resonant strips (MRS) configuration.

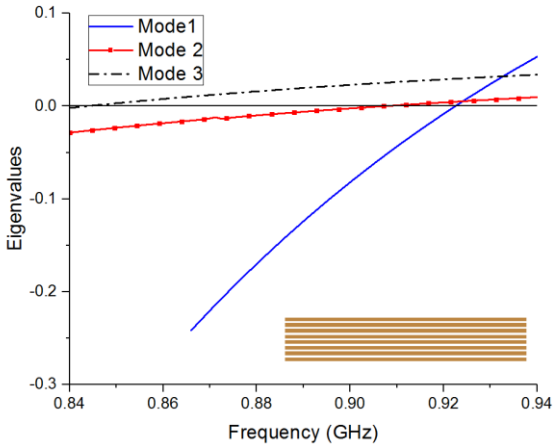

Fig. 4. Eigenvalue plot of multi-resonant strips configuration on PEC.

As a result, the gap between MRSs becomes 0.5 mm and 1 mm respectively due to the variable widths of MRS. The gap between the first and second MRS is 1 mm and next gap is 0.5 mm and so on. Fig. 4 shows the Eigenvalue plot of MRS configuration over perfect electric conductor (PEC) boundary conditions after setting optimal dimensions and gap values obtained using CST Microwave studio. It is clear from Fig. 4, that there are three resonating modes of resulting MRS configuration resonating at 925 MHz, 905 MHz, and 845 MHz. Modes 1 and 2 are resonating inside the US UHF RFID band and thus contributing towards bandwidth enhancement of the proposed RFID tag. Additionally, modes 1 and 2 help in achieving isolation from metal and other high permittivity surfaces.

The modal current distributions of the first two modes of MRS are shown in Fig. 5. The current distribution of mode 1 (resonating at 925 MHz) shows a current distribution similar to the current distribution of monopole. However, the mode 2 current distribution is similar to the current distribution of a loop.

The second layer of substrate with MRS configuration is proximity coupled and placed in parallel with SLT configurations. The distance between two layers is optimized using CST in order to get more number of modes in the required RFID band. Actually, the chip is attached to the first layer SLT, while the MRS configuration will act as a parasitic element. The Eigenvalues plot of the first three resonating modes of overall tag configuration is shown in Fig. 6. The optimal distance between layers or air gap is found to be 2.5 mm. The distance lesser than 2.5 mm creates a forced interruption in current patterns and hence on the resonance values of modes. Moreover, the distance of more than 2.5 mm up to 4 mm increases more number of resonant modes around 860 MHz.

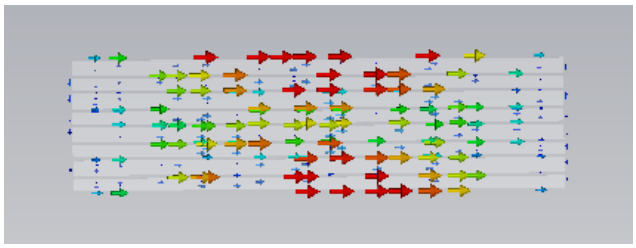

Mode 1

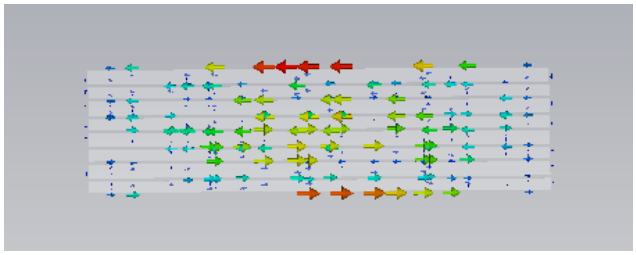

Mode 2

Fig. 5. Modal current distribution associated with first two modes of MRS configuration.

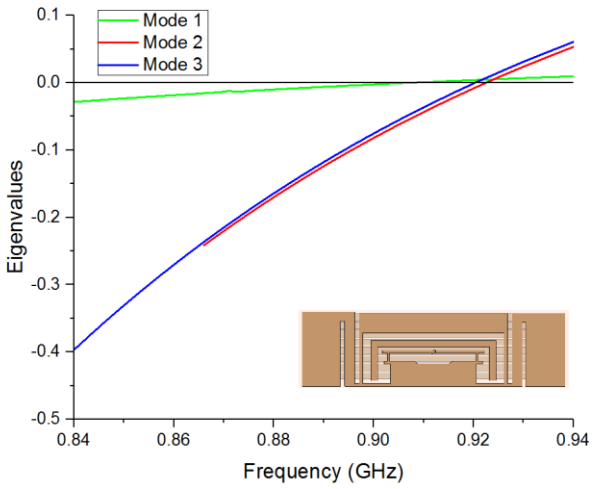

Fig. 6. Eigenvalue plot of first three modes of overall tag configuration on PEC.

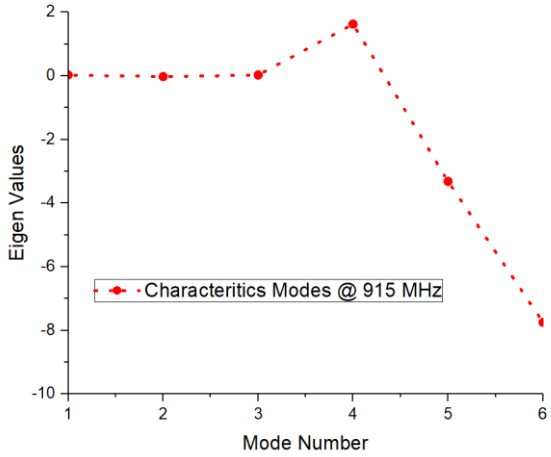

Fig. 7. Eigenvalue plot of six modes of overall tag configuration.

As can be seen from Fig. 6, there are three resonating modes resonating around 905 MHz, 915 MHz, and 925 MHz. All three modes contribute towards bandwidth enhancement of overall tag configuration.

Fig. 7 illustrates the eigenvalues plot of the first six modes of overall tag configuration. The first three modes are resonating in the required RFID band, while modes 4, 5, and 6 are non-resonating. Mode 4 expresses inductive behavior as its eigenvalue is greater than 0, while modes 5 and 6 express capacitive behavior as their eigenvalues are less than 0.

Fig. 8 shows the eigenvalue plot that describes the CM mode after placing SLT and MRS 1.5 mm apart. If we increase or decrease the distance, there will be a smaller number of modes in the required US UHF RFID band.

C. Antenna Configuration and Structure

Fig. 9 shows the detailed dimensions and structure of the complete tag configuration. The final antenna configuration consists of two layers of FR4 substrate separated by an air gap. The upper layer consists of the meandered dipole, T-match, and dual nested loop-based tag printed on a single-faced 0.5 mm substrate.

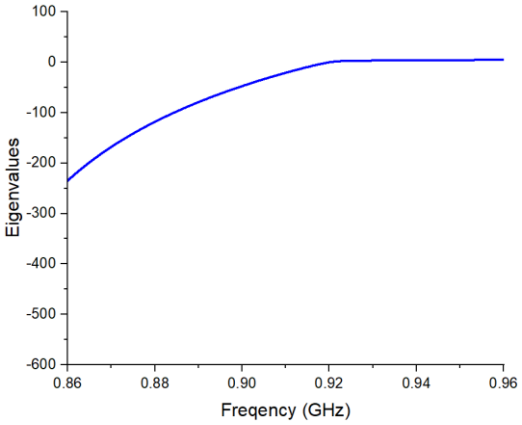

Fig. 8. Eigenvalue plot of CM modes after placing SLT and MRS 1.5 mm apart

The T-match and inverted u-shaped strip help to provide the best impedance match with the R6 RFID chip from the Impinj company. The lower substrate is equipped with MRS printed on a grounded 1 mm FR-4 substrate. The two adjacent strips have different widths, 2.5 mm and 2 mm, respectively. The gap between strips is 0.5 mm. Moreover, the two substrate layers are separated by an air gap of 2.5 mm. The Styrofoam 1 is mimicked in place of air in the fabricated prototype as its dielectric constant is near to air. The R6 RFID chip has an impedance of 14-140 j at 915 MHz estimated using Advanced Design System (ADS) by simulation equivalent circuit model given in datasheet of RFID chip. Table 1 shows the numerical values of the dimensions of the proposed design. The overall dimensions of this tag design are 85 mm × 28 mm × 4 mm. Moreover, it does not use any vias, shorting wall, or shorting pin, that make RFID tag designs expensive and difficult to fabricate.

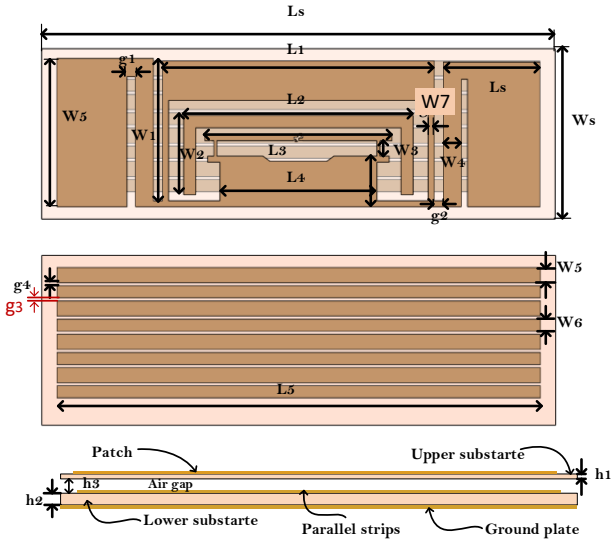

Fig. 9. Detailed dimensions and structure of overall tag configuration.

TABLE I
DIMENSIONS OF PROPOSED TAG

Dimension	Value (mm)	Dimension	Value (mm)	Dimension	Value (mm)
L_S	85	L_4	26	g_1	1.4
W_S	28	W_4	2.5	g_2	1.5
L_1	45	L_5	16	g_3	1
W_1	22.8	W_5	24.2	g_4	0.5
L_2	38	L_6	80	h_1	0.5
W_2	13	W_6	2.5	h_2	1
L_3	29	W_7	2	h_3	2.5
W_3	4	W_8	1		

III. DESIGN RESULTS AND MEASUREMENTS

Fig. 10 illustrates the simulated and measured S11 plot of the only upper layer and overall tag design. This upper layer of tag antenna does not work for metal or other high permittivity materials as its S11 plot is less than -3 dB. However, the S11 plot of the overall tag design with MRS depicts good performance in terms of bandwidth as it covers 900 MHz - 940 MHz. The intervention of MRS contributes to multiple modes that resulted in increased isolation and bandwidth enhancement even in the presence of a metallic environment (200 × 200 mm^2 metal plate). The associated simulated impedance plot of tag design after mounting on different surfaces is shown in Fig. 11.

It is clear from Fig. 11, that there is no obvious difference in impedance of the tag antenna after mounting on different surfaces such as air, metal, and the human body. For the human body, a four-layer model was used for simulation proposes. The four layers contain Skin, Muscle, Bone, and organ [23]. The simulated real impedance ranges from 12 Ω to 20 Ω with frequency bands ranging from 900 MHz to 940 MHz. Similarly, the simulated imaginary part of impedance has a value between 135 Ω to 150 Ω. This impedance performance of the tag antenna provides a good impedance match with the R6 RFID chip (14-140 j).

In order to investigate the performance and robustness of tag design further, the simulated S11 of the proposed tag antenna was observed for different sizes of metallic plates as depicted in Fig. 12. There was no considerable difference recorded ever after testing the size of more than 800 × 800 mm^2. The S11 plot shows the same performance in terms of bandwidth for all simulated sizes of metal plates such as 200 × 200 mm^2, 400 × 400 mm^2, and 600 × 600 mm^2.

To validate the simulation results, a prototype of the proposed tag antenna is fabricated for the measurement proposes as shown in Fig. 13. The impedance measurement setup is shown in Fig. 14, which contains Vector Network Analyzer (VNA) connected to a laptop equipped having MATLAB software. Moreover, a two-port probe formed using the port extension technique was used for impedance measurement of the tag. The probe is produced by joining the outer conductive shielding of two coaxial cables. The two inner ends of coaxial cables are differentially attached to each end of the tag antenna for impedance matching by following the procedure mentioned in [24].

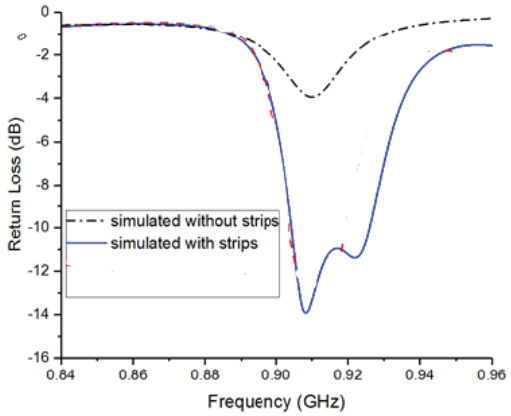

Fig. 10. The simulated plot of the only upper layer and overall tag design after mounting on a metal plate.

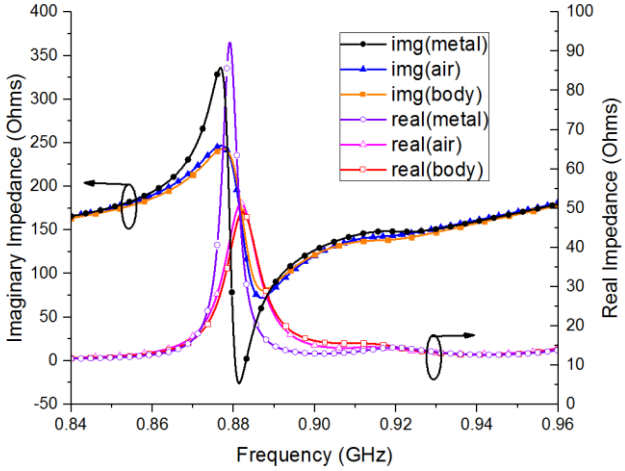

Fig. 11. Simulated impedance plot of overall tag configuration after mounting over different surfaces.

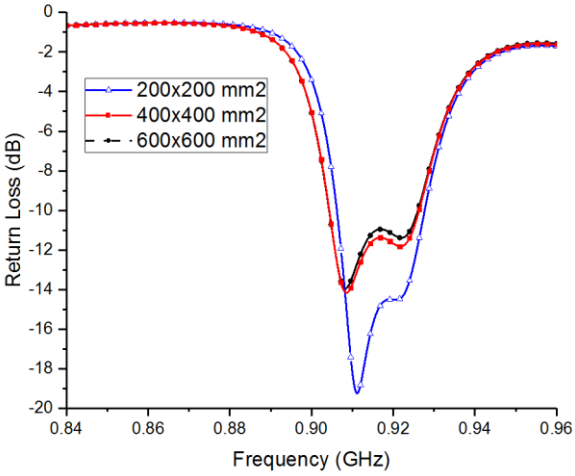

Fig. 12 Simulated S11 plot of tag antenna with different metal plate sizes.

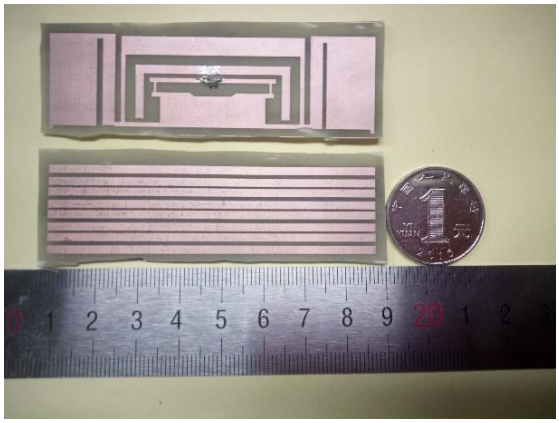

Fig. 13. Fabricated Prototype of MRS-based tag antenna.

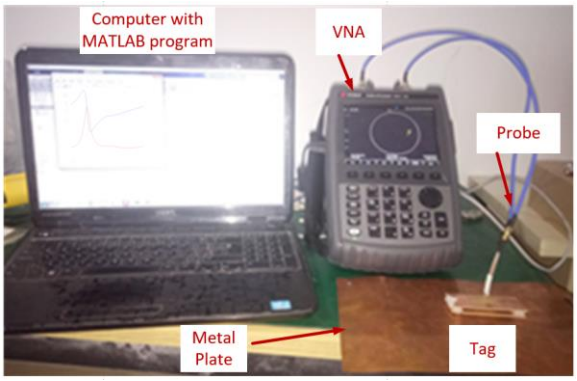

Fig. 14. Impedance measurement setup using Vector Network Analyzer and two-port Probe

Fig. 15 describes the measured real and imaginary impedance of tag design after mounting over 200 × 200 mm^2 metal plate. The imaginary part of the measured impedance is between 135 Ω to 155 Ω. Correspondingly, the measured real impedance also ranges from 10 Ω to 20 Ω. The measured impedance shows good compliance with simulated results as well as the impedance of the R6 RFID chip. The measured impedance depicts a bandwidth of 900 MHz- 935 MHz. The little discrepancy in measured results may be due to some fabrication error.

Fig. 15 shows the normalized radiation pattern of tag design along xz- and yz- planes at 915 MHz after placing over a metal plate. The radiation pattern shows maximum radiation of the antenna along +z direction.

To prove it further, the fabricated prototype of the tag antenna is connected with an RFID chip for read range measurement purposes. The theoretical read range estimation using the Friis equation is not so accurate.

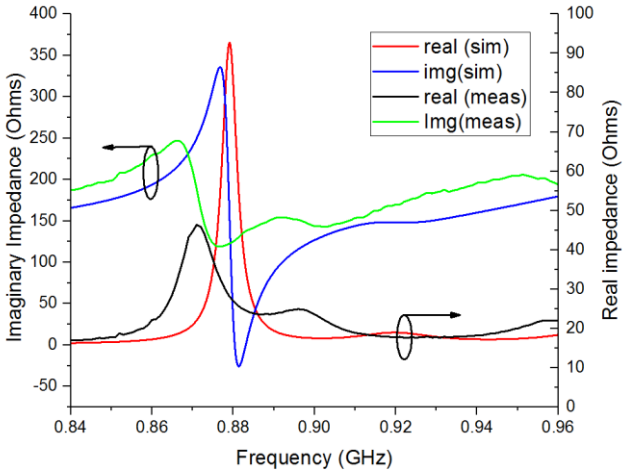

Fig. 15. Comparison of the simulated and measured impedance of proposed MRS-based tag antenna design.

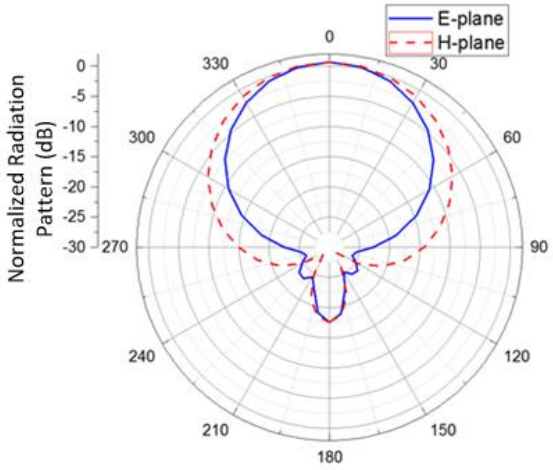

Fig. 16. Simulated normalized Radiation pattern along xz and yz planes at 915 MHz.

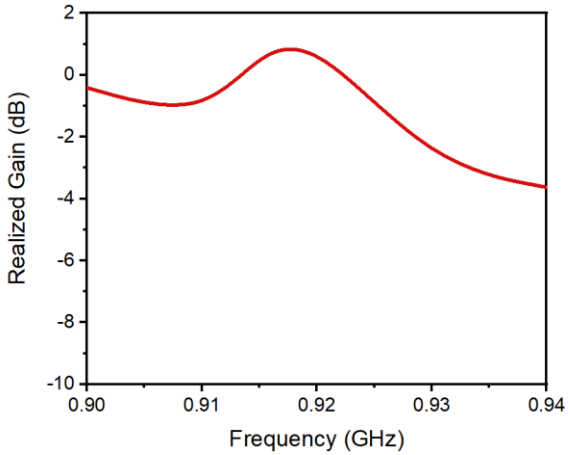

Fig. 17. Simulated gain of proposed MRS-based tag design

TABLE II
COMPARISON OF PROPOSED TAG ANTENNA WITH OTHER TAG DESIGN

Reference	This Work	[20]	[13]	[25]	[26]	[27]	[12]
Tag Size (mm)	85×28×4	55×41×3	47× 21 × 2.36	31.5 × 31.5 × 3.2	86×41×3.2	60.9×57.72×1.5	28.02 × 25.02 × 2.61
Bandwidth (MHz)	900 – 940	910 – 915	865– 960	858.9 – 869.7	840 – 900	915 – 920	910 – 915
Metal Plate Size (mm^2)	200×200	200×200	200×200	200×200	200×200	200×200	250×250
On metal Read Range (m)	14	14	4	7.25	5.6	8.4	8.1
Read range on low permittivity (εr<6) materials (m)	13	6.1	N.A	N.A	8	6.2	N.A
Read range on human body (m)	8.5	N.A	N.A	N.A	--	--	N.A

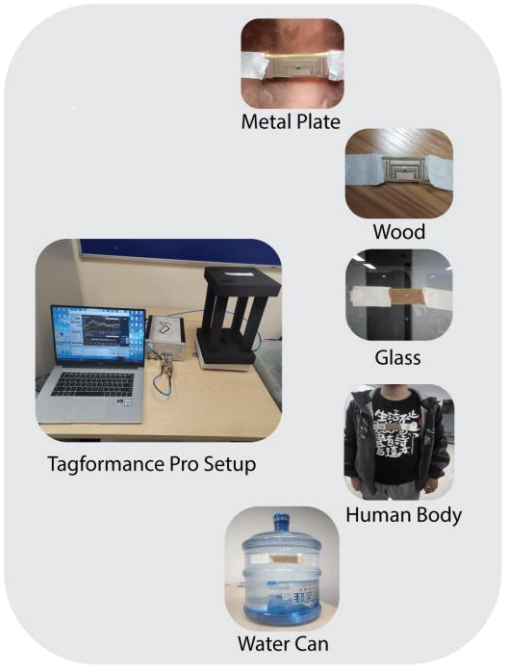

Fig. 18. Read range measurement setup using Tagformance Pro.

The simulated gain of the proposed MRS-tag is shown in Fig. 18. The gain is estimated after placing the tag over a 200 × 200 mm^2 metal plate. The maximum simulated gain of 1.1 dB was achieved at 922 MHz. The read range measurement setup using Tagformance Pro from Voyantic company is shown in figure 17. This setup includes a Tagformance Pro device, a transceiver antenna, a foam spacer, and a laptop with Tagformance software. The Tagformance setup works on a more accurate technique by determining the maximum read range for maximum permitted EIRP (Effective isotropic radiated power). The maximum read range is estimated by measuring read range for smaller EIRP described as follows:

$$R_{Max} = R_{reference}\sqrt{\frac{EIRP_{\max}}{EIRP_{ref}}} \quad (5)$$

Where R_{Max} and $EIRP_{max}$ are the maximum read range and maximum permitted EIRP (4W for most of the regions), respectively. While $R_{reference}$ and $EIRP_{ref}$ are the reference distance for read range measurement and reference EIRP of read range measuring equipment such as Tagformance.

The proposed tag has been mounted on different environmental surfaces such as wooden block, metal plate, glass piece, human body, and 19 Liter plastic water bottles. The read range testing sample with tag antenna is separated by a form spacer (30 cm). Fig. 19 shows the measured read range of the MRS-based tag design after employing different materials. This tag antenna achieved a read range of 15 m in air and 14 m on Metals. While, the read range recoded on glass, wood, and other low permittivity surfaces is 13.5 m. However, the suggested tag design expresses an 8 m read range both on the human body and water can. The reduced read range on the human body and water bottle is due to conductivity and the high dielectric constant of water and human tissues that reduces the radiation efficiency of the proposed tag design.

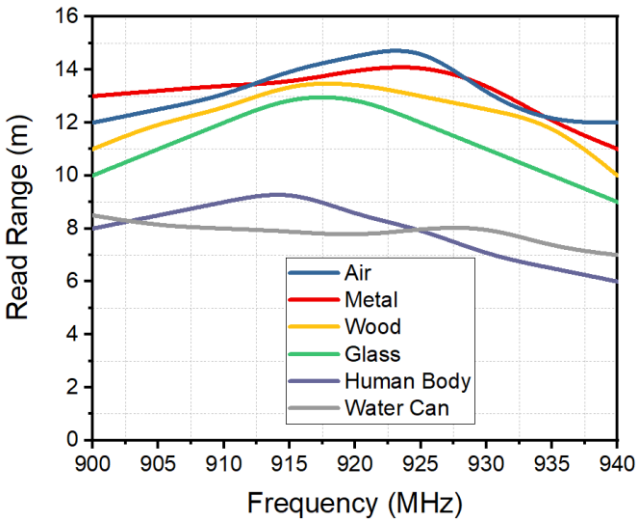

Fig. 19. The measured read range of MRS-based tag antenna after placing over different environment surfaces.

Table II shows the comparison of the proposed tag antenna with other state-of-the-art tag designs. The tag proposed in [20] shows a read range of 14 m and 6.1 m on the metal plate and other low permittivity substrates, respectively. However, this tag design has a substrate of 3 mm thickness with a very small bandwidth. The tag antenna proposed in [13] is smaller in size with wide bandwidth. However, this tag design offers a read range of 4 m only, without read range testing on other materials and the human body.

Another stacked inverted L tag antenna offers a very narrow bandwidth with a smaller footprint and read range of 7.25 m. The tag presented in [26], offers a read range of 5.6 m with a relatively large footprint. An inductively coupled tag design provides a read range of 8.4 m with a very narrow bandwidth. Similarly, a small shorted patch antenna was presented in [12]. This tag offers a read range of 8.1 m on the metal plate with 250 × 250 mm^2.

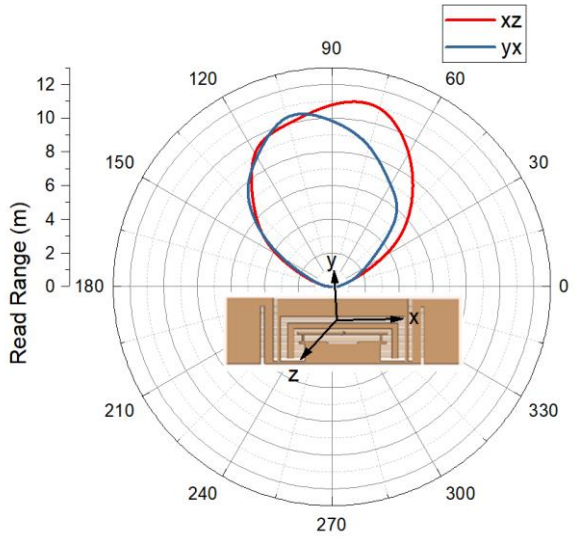

Fig. 20. Application of proposed tag antenna as car DNA after mounting on the license number plate and toll payment

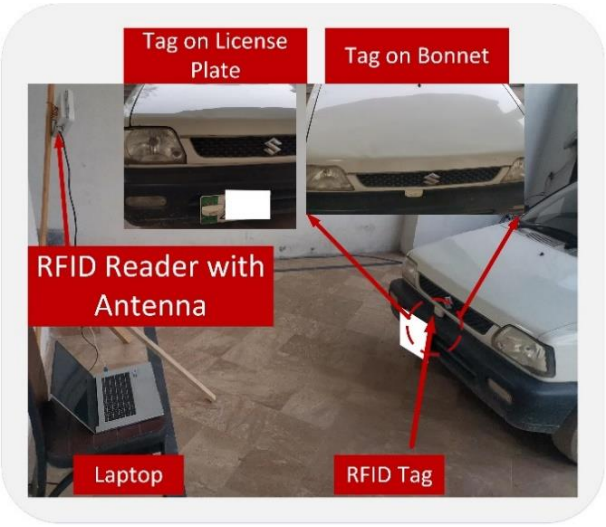

Fig. 21. Application of proposed tag antenna as car DNA after mounting on the license number plate and toll payment.

Since the proposed tag provides a good read range of more than 14 m after mounting on the metal plate with a size of 200 × 200 mm^2. Moreover, it provides a read range of more than 13.5 m on different materials. In addition, the proposed tag design offers a bandwidth of 900 MHz to 940 MHz on all materials, which makes it suitable for harsh environments and platform tolerability. The read range pattern of tag design at various angles is presented in Fig. 20 after mounting on the metal plate. To prove it further, the proposed tag antenna is tested by placing it at different locations of a car. The tag antenna is mounted on three different locations (i) license number plate (ii) plastic Bumper (iii) metallic part of the bonnet. Fig. 21 shows the read range measurement setup of the application scenario. This tag achieved a read range of more than 10 m on all three locations. Therefore, this tag antenna can be used as a car's DNA, which can be further used for toll payment or other parking fees as well as security purposes.

IV. Conclusion

A wideband, long-range tag antenna with platform tolerant features is proposed using CMA. This tag design consists of two layers. The proposed tag antenna is backed by a multi-resonant surface to provide isolation and multi-resonant modes, that enhance the bandwidth of tag design on different environment surfaces. The tag antenna achieved a read range of 15 m, 14 m, and 13.5 in free space, on the metal plate and other materials (glass, wood). Moreover, it offered a read range of 8 m on the human body. In addition to this, the proposed tag antenna provides a wide bandwidth ranging from 900 -940 MHz, that covers both US, Chinese, and upper European RFID bands. Furthermore, the proposed antenna was also tested in a harsh metal environment such as car number plates and cargo metallic containers. Therefore, the proposed tag can be used for tagging metallic containers, wood containers, and other harsh platforms for cargo management, Asset tracking, supply chain visibility, and Internet of Things (IoT) Applications.

Acknowledgment

This work is supported by the Ajman University Internal Research Grant.

References

[1] T. Athauda, J. C. L. Marin, J. Lee, and N. C. Karmakar, "Robust Low-Cost Passive UHF RFID Based Smart Shopping Trolley," *IEEE J. Radio Freq. Identif.*, vol. 2, no. 3, pp. 134–143, 2018, doi: 10.1109/JRFID.2018.2866087.

[2] A. Sharif *et al.*, "Low-cost inkjet-printed UHF RFID tag-based system for internet of things applications using characteristic modes," *IEEE Internet Things J.*, vol. 6, no. 2, pp. 3962–3975, Apr. 2019, doi: 10.1109/JIOT.2019.2893677.

[3] E. Perret, S. Tedjini, and R. S. Nair, "Design of antennas for UHF RFID tags," *Proc. IEEE*, vol. 100, no. 7, pp. 2330–2340, 2012, doi: 10.1109/JPROC.2012.2186950.

[4] A. Dinatale, A. Dicarlofelice, and E. Digiampaolo, "A Crack Mouth Opening Displacement Gauge Made with Passive UHF RFID Technology," *IEEE Sens. J.*, vol. 22, no. 1, pp. 174–181, Jan. 2022, doi: 10.1109/JSEN.2021.3130064.

[5] K. Zannas, H. El Matbouly, Y. Duroc, and S. Tedjini, "A Flipping UHF RFID Sensor-Tag for Metallic Environment Compliant with ETSI/FCC Bands," *IEEE Trans. Antennas Propag.*, vol. 69, no. 3, pp. 1283–1292, 2021, doi: 10.1109/TAP.2020.3026869.

[6] Y. H. Lee, C. W. Moh, E. H. Lim, F. L. Bong, and B. K. Chung, "Miniature Folded Patch with Differential Coplanar Feedline for Metal Mountable UHF RFID Tag," *IEEE J. Radio Freq. Identif.*, vol. 4, no. 2, pp. 93–100, 2020, doi: 10.1109/JRFID.2019.2957011.

[7] Y. H. Niew, K. Y. Lee, E. H. Lim, F. L. Bong, and B. K. Chung, "Miniature Dipolar Patch Antenna with Nonresonating Ring for Metal-Insensitive UHF RFID Tag Design," *IEEE Trans. Antennas Propag.*, vol. 68, no. 3, pp. 2393–2398, 2020, doi: 10.1109/TAP.2019.2940521.

[8] S. R. Lee, E. H. Lim, F. L. Bong, and B. K. Chung, "High-Efficient Compact Folded-Patch Antenna Fed by T-Shaped L-Probe for On-Metal UHF RFID Tag Design," *IEEE Trans. Antennas Propag.*, vol. 68, no. 1, pp. 152–160, 2020, doi: 10.1109/TAP.2019.2938794.

[9] W. H. Ng, E. H. Lim, F. L. Bong, and B. K. Chung, "E-Shaped Folded-Patch Antenna with Multiple Tuning Parameters for On-Metal UHF RFID Tag," *IEEE Trans. Antennas Propag.*, vol. 67, no. 1, pp. 56–64, 2019, doi: 10.1109/TAP.2018.2874795.

[10] R. Abdulghafor *et al.*, "Recent Advances in Passive UHF-RFID Tag Antenna Design for Improved Read Range in Product Packaging Applications: A Comprehensive Review," *IEEE Access*, vol. 9, pp. 63611–63635, 2021, doi: 10.1109/ACCESS.2021.3074339.

[11] S. Y. Ooi, P. S. Chee, E. H. Lim, Y. H. Lee, and F. L. Bong, "Stacked Planar Inverted-L Antenna with Enhanced Capacitance for Compact Tag Design," *IEEE Trans. Antennas Propag.*, vol. 70, no. 3, pp. 1816–1823, Mar. 2022, doi: 10.1109/TAP.2021.3118822.

[12] M. T. Nguyen, Y. F. Lin, C. H. Chen, C. H. Chang, and H. M. Chen, "Shorted patch antenna with multi slots for a UHF RFID tag attached to a metallic object," *IEEE Access*, vol. 9, pp. 111277–111292, 2021, doi: 10.1109/ACCESS.2021.3103177.

[13] S. R. Lee, E. H. Lim, and S. K. A. Rahim, "Small Wideband Antenna for On-Metal UHF RFID Tag Design," *IEEE J. Radio Freq. Identif.*, vol. 6, pp. 121–127, 2022, doi: 10.1109/JRFID.2021.3134492.

[14] D. Inserra and G. Wen, "Low profile metal tolerant UHF RFID tag with lumped elements for post-manufacturing frequency tuning," *IEEE Trans. Antennas Propag.*, vol. 69, no. 11, pp. 7953–7958, Nov. 2021, doi: 10.1109/TAP.2021.3083729.

[15] Y. H. Lee, C. W. Moh, E. H. Lim, F. L. Bong, and B. K. Chung, "Miniature Folded Patch with Differential Coplanar Feedline for Metal Mountable UHF RFID Tag," *IEEE J. Radio Freq. Identif.*, vol. 4, no. 2, pp. 93–100, Jun. 2020, doi: 10.1109/JRFID.2019.2957011.

[16] F. K. Byondi and Y. Chung, "Longest-range UHF RFID sensor tag antenna for iot applied for metal and non-metal objects," *Sensors (Switzerland)*, vol. 19, no. 24, p. 5460, Dec. 2019, doi: 10.3390/s19245460.

[17] Y. Yan, A. Sharif, J. Ouyang, C. Zhang, and X. Ma, "UHF RFID handset antenna design with slant polarization for IoT and future 5G enabled smart cities applications using CM analysis," *IEEE Access*, vol. 8, pp. 22792–22801, 2020, doi: 10.1109/ACCESS.2020.2970254.

[18] T. Althobaiti, A. Sharif, J. Ouyang, N. Ramzan, and Q. H. Abbasi, "Planar Pyramid Shaped UHF RFID Tag Antenna with Polarisation Diversity for IoT Applications Using Characteristics Mode Analysis," *IEEE Access*, vol. 8, pp. 103684–103696, 2020, doi: 10.1109/ACCESS.2020.2999256.

[19] A. Sharif, J. Ouyang, F. Yang, R. Long, and M. K. Ishfaq, "Tunable Platform Tolerant Antenna Design for RFID and IoT Applications Using Characteristic Mode Analysis," *Wirel. Commun. Mob. Comput.*, vol. 2018, 2018, doi: 10.1155/2018/9546854.

[20] H. Li, J. Zhu, and Y. Yu, "Compact Single-Layer RFID Tag Antenna Tolerant to Background Materials," *IEEE Access*, vol. 5, pp. 21070–21079, 2017, doi: 10.1109/ACCESS.2017.2756670.

[21] M. Cabedo-Fabres, E. Antonino-Daviu, A. Valero-Nogueira, and M. F. Bataller, "The theory of characteristic modes revisited: A contribution to the design of antennas for modern applications," *IEEE Antennas Propag. Mag.*, vol. 49, no. 5, pp. 52–68, 2007, doi: 10.1109/MAP.2007.4395295.

[22] Y. Chen and C. F. Wang, *Characteristic Modes: Theory and Applications in Antenna Engineering*. wiley, 2015.

[23] S. Amendola, S. Milici, and G. Marrocco, "Performance of Epidermal RFID Dual-loop Tag and On-Skin Retuning," *IEEE Trans. Antennas Propag.*, vol. 63, no. 8, pp. 3672–3680, 2015, doi: 10.1109/TAP.2015.2441211.

[24] X. Qing, C. K. Goh, and Z. N. Chen, "Impedance characterization of rfid tag antennas and application in tag co-design," *IEEE Trans. Microw. Theory Tech.*, vol. 57, no. 5, pp. 1268–1274, 2009, doi: 10.1109/TMTT.2009.2017288.

[25] S. Y. Ooi, P. S. Chee, E. H. Lim, Y. H. Lee, and F. L. Bong, "Stacked Planar Inverted-L Antenna with Enhanced Capacitance for Compact Tag Design," *IEEE Trans. Antennas Propag.*, vol. 70, no. 3, pp. 1816–1823, 2022, doi: 10.1109/TAP.2021.3118822.

[26] A. P. Sohrab, Y. Huang, M. N. Hussein, and P. Carter, "A Hybrid UHF RFID Tag Robust to Host Material," *IEEE J. Radio Freq. Identif.*, vol. 1, no. 2, pp. 163–169, 2017, doi: 10.1109/JRFID.2017.2765623.

[27] F. Erman *et al.*, "U-Shaped Inductively Coupled Feed UHF RFID Tag Antenna with DMS for Metal Objects," *IEEE Antennas Wirel. Propag. Lett.*, vol. 19, no. 6, pp. 907–911, Jun. 2020, doi: 10.1109/LAWP.2020.2981960.

ABUBAKAR SHARIF received the M.Sc. degree in electrical engineering from the University of Engineering and Technology, Lahore, Pakistan, and the Ph.D. degree in electronics engineering from the University of Electronic Science and Technology of China (UESTC). From 2011 to 2016, he worked as a Lecturer with Government College University Faisalabad (GCUF), Pakistan. He is also working as a Research Fellow with UESTC. He is the author of several peer-reviewed international journal and conference papers. His research interests include wearable and flexible sensors, compact antenna design, antenna interaction with the human body, antenna and system design for RFID, phased array antennas, passive wireless sensing, and the Internet of Things (IoTs).

JUN OUYANG received the Ph.D. degree in electromagnetic and microwave technology from the University of Electronic Science and Technology of China (UESTC), in 2008, and the Post doctorate degree in information and signal processing from UESTC, in 2011. He is currently working as an Associate Professor with the School of Electronic Science and Engineering, UESTC. He is also the Associate Director of the Smart Cities Research Center, UESTC. He is also a Research Fellow and the Chief Scientist of the Internet of Things Technology with the Chengdu Research Institute. He is the author of more than 80 articles and 20 patents. Recently, he is leading several national-level research projects, provisional and ministerial research projects. His research interests include antenna theory and design, microwave system, RFID tag, wireless sensing, and the Internet of Things.

KAMRAN ARSHAD (SM'15) is currently the Dean of Research and Graduate Studies and a Professor in electrical engineering with Ajman University, United Arab Emirates. Prior to join Ajman University, in January 2016, he has been Associated with the University of Greenwich, U.K., as a Senior Lecturer and the Program Director of M.Sc. Wireless Mobile Communications Systems

Engineering. He is also a Senior Fellow of the U.K. Higher Education Academy (SF-HEA). He is an Associate Editor of the EURASIP Journal on Wireless Communications and Networking. He led a number of locally and internationally funded research projects encompassing the areas of cognitive radio, LTE/LTE-Advanced, 5G, Optimization and cognitive Machine-to-Machine (M2M) communications. He has contributed to several European and international large-scale research projects. He has over 130 technical peer-reviewed articles in top quality journals and international conferences, received three Best Paper Awards, one best Research and Development Track Award, and chaired technical sessions in several leading international conferences.

Dr. Khaled Assaleh is currently the Vice Chancellor for Academic Affairs and a Professor of Electrical Engineering at Ajman University. From 2002 through 2017, he was with the American University of Sharjah (AUS) as a Professor of Electrical Engineering and Vice Provost for Research and Graduate Studies. Prior to joining AUS, Khaled had a 9-year R&D career in the Telecom Industry in the USA with Rutgers, Motorola and Rockwell/Skyworks. He earned a Ph.D. in Electrical Engineering from Rutgers, the State University of New Jersey in 1993; a Master's degree in Electronic Engineering from Monmouth University, New Jersey in 1990; and a B.Sc. in Electrical Engineering from the University of Jordan in 1988. He holds 11 US patents and has published over 120 articles in signal/image processing and pattern recognition and their applications. He has served on organization committees of several international conferences including ICIP, ISSPA, ICCSPA, MECBME and ISMA. He has also served as a guest editor for several special issues of journals. Dr. Assaleh is a senior member of the IEEE. His research interests include bio-signal processing, biometrics, speech and image processing, and pattern recognition.

MUHAMMAD ALI IMRAN (SM 12) received the M.Sc. (Hons.) and Ph.D. degrees from Imperial College London, U.K., in 2002 and 2007, respectively. He is Dean University of Glasgow UESTC and a Professor of communication systems with the James Watt School of Engineering, University of Glasgow. He is an Affiliate Professor at the University of Oklahoma, USA, and a Visiting Professor at the 5G Innovation Centre, University of Surrey, U.K. He is leading research in University of Glasgow for Scotland 5G Center. He has over 18 years of combined academic and industry experience, working primarily in the research areas of cellular communication systems. He has been awarded 15 patents, has authored/co-authored over 500 journal and conference publications, and has been principal/co-principal investigator on over £8 million in sponsored research grants and contracts. He has supervised 40+ successful Ph.D. graduates. He has an award of excellence in recognition of his academic achievements, conferred by the President of Pakistan. He was also awarded the IEEE Comsoc's Fred Ellersick Award 2014, the FEPS Learning and Teaching Award 2014, and the Sentinel of Science Award 2016. He is a shortlisted finalist for The Wharton-QS Stars Awards 2014, the QS Stars Reimagine Education Award 2016 for innovative teaching, and VC's Learning and Teaching Award from the University of Surrey. He is a Senior Fellow of the Higher Education Academy, U.K. He is the editor/co-editor of 8 books.

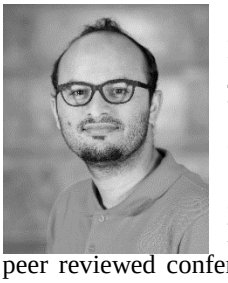

Qammer H. Abbasi (Senior Member, IEEE) is currently a Reader with the James Watt School of Engineering, University of Glasgow, Glasgow, U.K., and the Deputy Head for Communication Sensing and Imaging Group. He has authored or coauthored more than 350 leading international technical journal and peer reviewed conference papers and ten books. He was the recipient of several recognitions for his research, including URSI 2019 Young Scientist Awards, U.K. exceptional talent endorsement by Royal Academy of Engineering, Sensor 2021 Young Scientist Award, National talent pool award by Pakistan, International Young Scientist Award by NSFC China, National interest waiver by USA and eight best paper awards. He is a Committee Member of IEEE APS Young professional, Sub-committee Chair of IEEE YP Ambassador program, IEEE 1906.1.1 standard on nano communication, IEEE APS/SC WG P145, IET Antenna & Propagation, and healthcare network. He is also a member of IET and a Fellow of RET and RSA.